Passivating Silicon Grain Boundaries with Small Polar Molecules for Photovoltaics

Wentao Wang[1], Fude Liu[1,*], Lei Wang[1], Guandong Yang[1], Wallace C.H. Choy[2], Fei Yan[3], Steven Johnston[3] and Mowafak M. Al-Jassim[3]

[1]*Department of Mechanical Engineering, The University of Hong Kong, Hong Kong, China*

[2]*Department of Electrical and Electronic Engineering, The University of Hong Kong, Hong Kong, China*

[3]*National Center for Photovoltaics, National Renewable Energy Laboratory, Golden, CO 80401, USA*

Abstract: Grain boundaries (GBs) play a major role in determining the device performance of in particular polycrystalline thin-film solar cells. Hydrogen has traditionally been applied to passivate defects at GBs. However, hydrogenated films are subject to light-induced degradation effects. In this study, we took a novel approach to passivating GBs in multicrystalline silicon (mc-Si) wafers with small polar molecules. We found an excellent correlation between the grain misorientation, electrical resistance across GBs, and passivation effectiveness. In particular, the charge transport across GBs was greatly enhanced after the wafers were properly treated in our polar molecule solutions; the sheet resistance can be reduced by up to more than one order for large-angle random GBs. The results were explained to be due to the effective charge neutralization and passivation of polar molecules on localized charge states at GBs. These findings may help us achieve high-quality materials at low cost for high-efficiency solar cells by enhancing carrier transport and minimizing carrier recombination.

Keywords: Passivation, Photovoltaics, Polar molecules, Grain boundaries, Silicon.

1. INTRODUCTION

Silicon is the workhorse material of the photovoltaics industry, and the thin-film polycrystalline silicon (*poly*-Si) with grain size in the range of 1 µm to 1 mm is considered a promising emerging technology because of their potential for low cost among other benefits [1-3]. However, grain boundaries (GBs) are a significant concern because they play a major role in determining the device performance of these polycrystalline thin-film solar cells [4-6]. The high density defects in GBs act as recombination centers to trap the minority flow carriers. To minimize the effect of GBs, the key is to either eliminate them or eliminate their electrical activity [7]. The latter approach of GB passivation is considered to be more feasible and economical. Hydrogen has traditionally been applied to passivate the defects at GBs. It was first studied through introducing hydrogen plasma in bulk *poly*-Si GBs, and effectively reduced GB in-gap states and potential barrier [8]. Extensive studies on hydrogenation technique as well as mechanisms behind were conducted on thin film *poly*-Si, and *mc*-Si [5,9-14]. However, hydrogenated films are subject to the low thermal stability [15,16]. Furthermore, excessive hydrogenation leads to new defect creation and results in the increase of GB electrical activity in *poly*-Si [17,18]. Alternative passivation agents are therefore developed. Molecules with polarity such as NH_3, and H_2O were observed to eliminate the GB trap states in *poly* Si [7,19]. However, the gas diffusion treatment at high temperature is expensive to maintain. A feasible solution can be achieved with chemical passivation. For example, immersing hydrogen terminated silicon substrate in quinhydrone-methanol solution can obtain surface passivation effect and higher minority carrier lifetime [20,21].

In this study, we suggest a novel approach using small polar molecules (methanol, acetonitrile, formic acid, and new ZK-series mixed solutions) by chemical solution process to passivate GBs in *poly*-Si and multicrystalline silicon (*mc*-Si) wafers. This low temperature passivation method has advantages in the operation simplicity and low requirement on process condition. Moreover, this method in principle can be applied to other polycrystalline thin-film solar cells, including cadmium telluride (CdTe), copper indium gallium selenide (CIGS), and copper zinc tin sulfide (CZTS). In the present investigation, the large-angle random “GBs” electrical activity can be significantly reduced by up to more than one order in *mc*-Si. In addition, the correlation of GB microstructure with passivation effect was well investigated. *mc*-Si wafers rather than polycrystalline thin films were chosen because of their large grains, which make it easier to practically study the GB behaviors. This simple passivation method with small molecules is promising

---

*Address correspondence to this author at the Department of Mechanical Engineering, The University of Hong Kong, Hong Kong, China;
Tel: (+852) 2859-2631; Fax: 2858-5415; E-mail: fordliu@hku.hk

E-ISSN: 2410-2199/14

in achieving high quality materials at low cost and improving energy conversion performance for photovoltaics.

2. MATERIALS AND METHODS

Investigation was carried out on *p*-type *mc*-Si wafers (thickness: ~200 um; resistivity: 0.5–3 Ω·cm; grain size: mm–cm). Wafers were first cut into small samples of a few cm. GBs marked lightly with a diamond scribe were examined in detail to see sheet resistance changes before and after passivation. All samples were cleaned using the standard Radio Corporation of America (RCA) clean procedure, followed by etching in 1:50 hydrofluoric acid for 30 seconds, rinsing with deionized water for 1 minute, and then drying with compressed air. The passivation was then conducted by immersing cleaned samples in methanol (CH_3OH), formic acid ($HCOOH$), acetonitrile (CH_3CN), and our home-made ZK-series polar molecule solutions, respectively, at a fixed temperature (<100°C) for certain periods of time. Passivated samples were then taken out, dried with compressed air, and left in air at room temperature for more than 12 hours before measuring the sheet resistance with a four-point probe station (Signatone S-301-4). The resistance measurement was conducted across GBs and on grain bulk, respectively, under both dark and illuminated conditions. The light source was a standard solar simulator (ABET Sun 2000). The resistance across each GB was obtained by averaging several data points acquired along the GB. After finishing the resistance measurement, each sample was first RCA cleaned and then put back in the same chemical solution again for further passivation at an incremental step of 5 hours to study the effect of passivation time on the resistance. In addition, photoluminescence (PL) and electron backscatter diffraction (EBSD) techniques were also applied to study the correlation between the electrical, optical, and structural properties of GBs. For PL imaging, the wafer was illuminated by 810 nm light at an intensity equivalent to one sun, and the data acquisition time was 600 seconds. The plan-view EBSD mapping was carried out with a scanning electron microscope (SEM) (Hitachi S-4300N) at 20 kV, a sample tilt angle of 70°, and a working distance of 15 mm. More details on PL and EBSD can be found elsewhere [22,23].

3. RESULTS AND DISCUSSION

We first studied the GB passivation with pure polar molecular solutions only. Figure **1** shows the sheet resistance (R_{sheet}) across GBs *vs.* passivation time on two kinds of GBs (large-angle random and Σ3) under dark (D = dark) and illuminated (L = light) conditions, respectively. The dipole moments of formic acid, methanol, and acetonitrile are 1.41, 1.69, and 3.9 D (D = Debye), respectively [24-26]. As shown in Figure **1a**, methanol is generally more effective in passivating large-angle random GBs than are formic acid and acetonitrile. In particular, after a 10-hour methanol passivation, the dark R_{sheet} and illuminated R_{sheet} values decreased from 5637.2 and 4317.2 Ω/□ to 3711.0 and 3196.5 Ω/□, respectively (or equivalently, by 34.2% and 26.0%, respectively). The relatively effective passivation of methanol might be related to its small molecule size of ~0.41 nm, [27] which makes it easier to diffuse along GBs for passivation and therefore lowers the energy potential barrier there. However, the

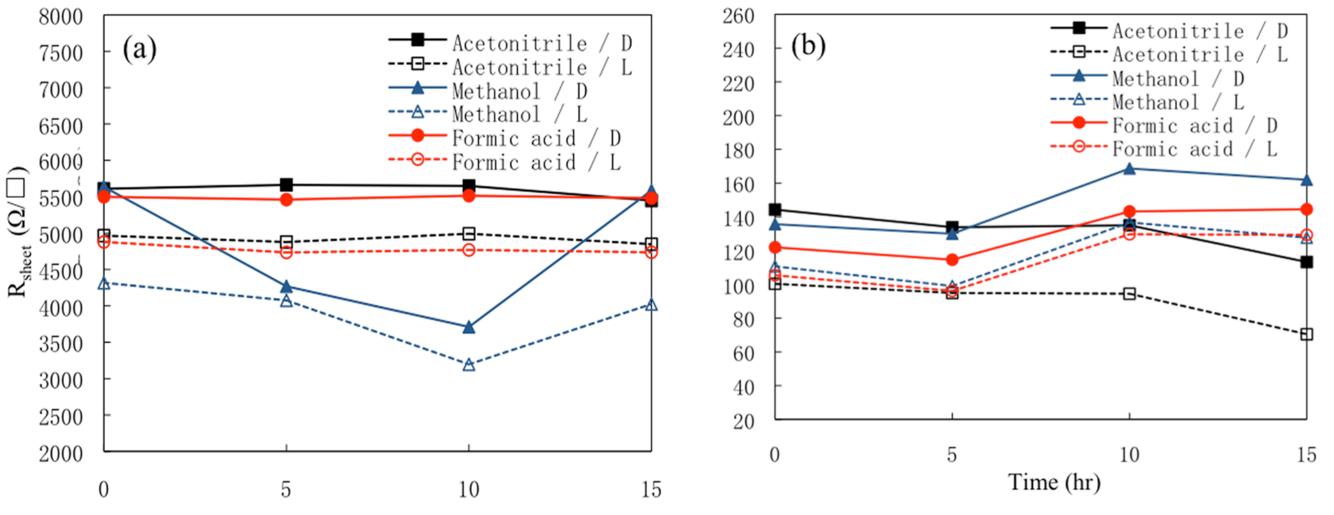

Figure 1: Sheet resistance (R_{sheet}) across GBs *vs.* passivation time of acetonitrile, methanol, and formic acid under dark (D) and illuminated (L) conditions, respectively. (**a**) Large-angle random GBs. (**b**) Σ3 GBs.

R_{sheet} almost returned to its original value when the passivation time was further increased. In contrast, the passivation of acetonitrile and formic acid on large-angle random GBs is not obvious for the entire range of treatment time under both dark and illuminated conditions. For instance, the dark R_{sheet} and illuminated R_{sheet} remained almost constant around 5500 and 4800 Ω/□, respectively, for large-angle random GBs treated with formic acid. For Σ3 GBs (Figure **1b**), R_{sheet} values are usually in the range of 60−180 Ω/□, which are much smaller than those of large-angle random GBs. We see that the passivation on Σ3 GBs did not greatly change the R_{sheet} values, although in general acetonitrile may reduce R_{sheet}, and methanol (or formic acid) may increase R_{sheet}. Overall, we can conclude that with appropriate small polar molecules, the electrical activity of GBs can be modified to a certain extent. However, the passivation effectiveness of pure molecule candidates on large-angle GBs is still limited. We then investigated the passivation performance of our ZK-series polar molecule solutions, whose dipole moments can be varied from 2.2 to 3.4 D.

As depicted in Figure **2a**, all three kinds of ZK-series solutions could effectively passivate large-angle random GBs and then greatly reduce their R_{sheet} values. For GBs passivated with ZK-22 solution, the corresponding R_{sheet} decreased dramatically even after the first 5 hours of passivation; the values of R_{sheet} dropped from 5804.9 and 5083.6 Ω/□ to 1144.6 and 848.3 Ω/□ under dark and illuminated conditions, respectively. With further passivation, the R_{sheet} increased slightly first and then dropped to saturation values of 180.4 and 176.2 Ω/□, respectively, under dark and illuminated conditions, when the passivation time reached 30 hours. We therefore see that the R_{sheet} across large-angle GBs could be reduced by more than 95% after ZK-22 passivation. Compared to ZK-22 solution, both the ZK-24 and ZK-42 solutions generally followed a similar trend in terms of passivation effectiveness on large-angle GBs. However, for GBs passivated with either the ZK-24 or ZK-42 solution, the corresponding R_{sheet} did not decrease significantly until the passivation reached 10 hours, and after that, the R_{sheet} saturated to low values (<1000 Ω/□), which makes both the ZK-24 and ZK-42 solutions better passivation candidates as far as the passivation time window is concerned. We also tested the conductivity of ZK-series solutions and found them to be insulating, which rules out the possibility that the resistance reduction after passivation was caused by the conductivity of the polar molecules themselves. We therefore think the improvement of the electrical properties at GBs is due to the interaction between mc-Si GBs and polar molecules. For Σ3 GBs passivated with ZK-series solutions, the R_{sheet} was generally not sensitive to the passivation (Figure **2b**), although it fluctuated to some extent, similar to the case of Σ3 GBs passivated with pure polar molecules as shown earlier in Figure **1b**. It is reasonable to assume that polar molecules did not have much effect on the electrical activity of Σ3 GBs because it is well known that Σ3 boundaries are structurally much less defective and thus almost electrically inactive [4,22]. We observed that all passivated samples showed very stable electrical resistance even when left in air at room temperature for four weeks. These findings are significant because the R_{sheet} values of defective random GBs can be greatly reduced to be close to the

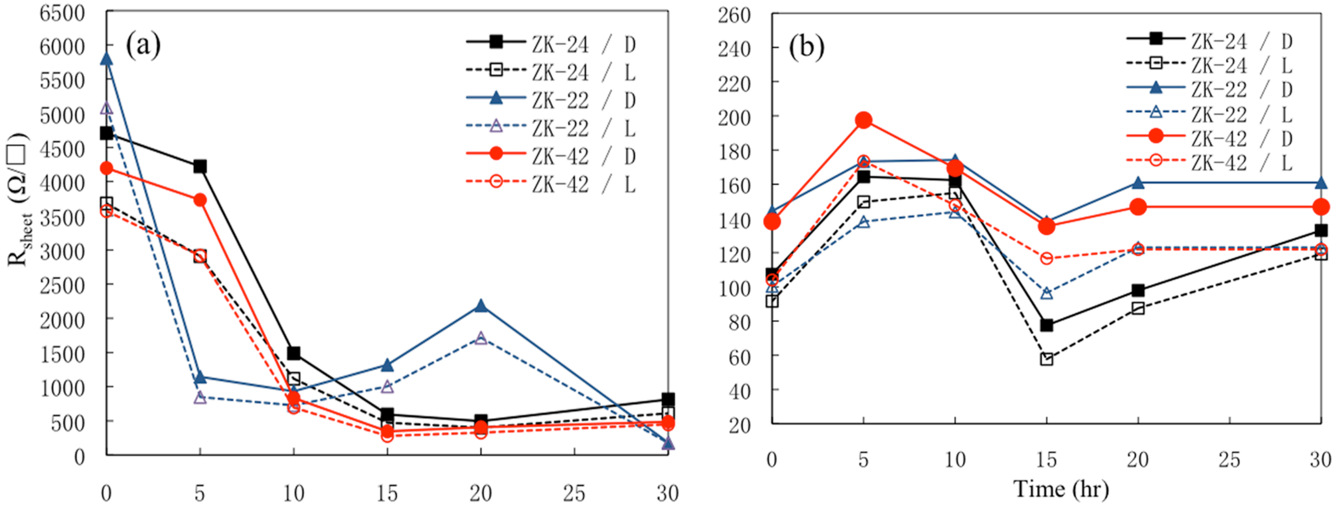

Figure 2: Sheet resistance (R_{sheet}) across GBs *vs.* passivation time of ZK-24, ZK-22, and ZK-42 under dark (D) and illuminated (L) conditions, respectively. (**a**) Large-angle random GBs. (**b**) Σ3 GBs.

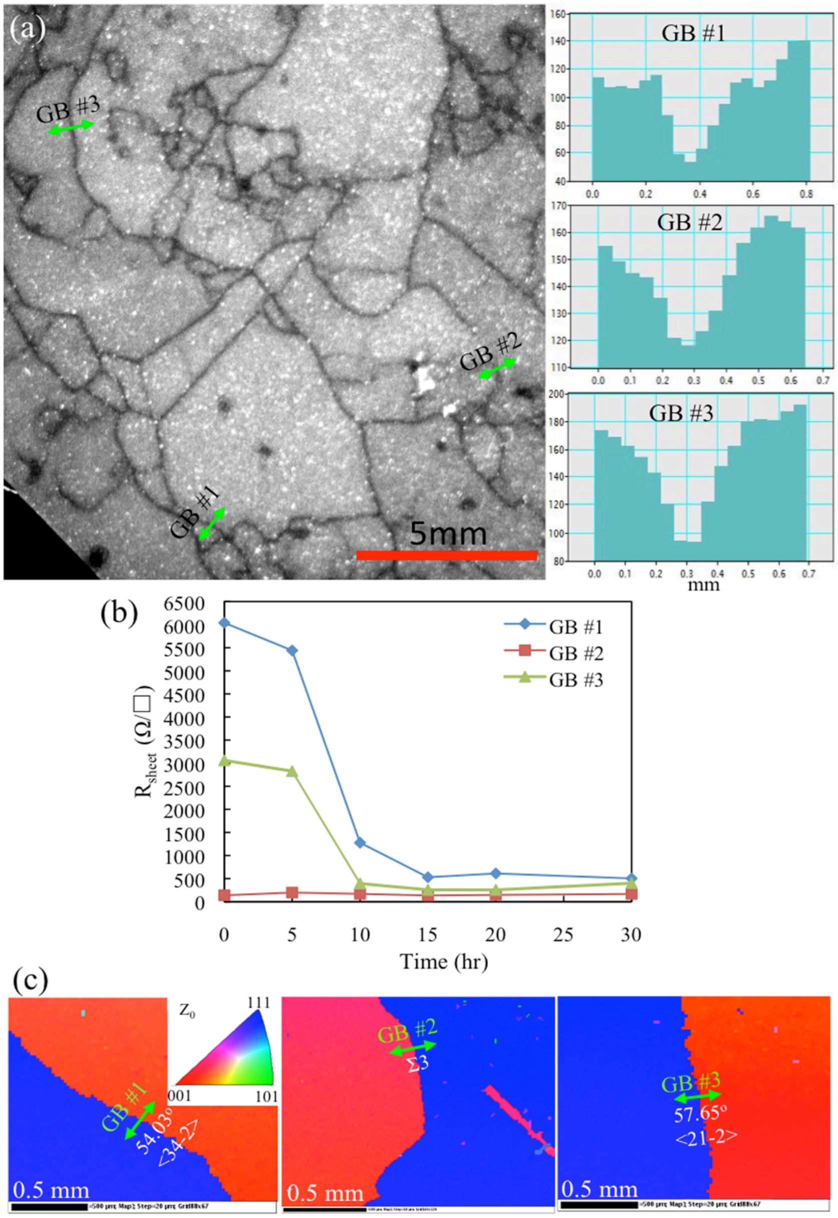

Figure 3: Sample passivated with ZK-42. (**a**) PL image of a sample passivated for 30 hours. The insets are the corresponding PL intensity profiles across GBs #1−3. (**b**) Sheet resistance (R_{sheet}) across GBs #1−3 *vs.* passivation time under dark condition. (**c**) Plan-view EBSD maps at GBs #1–3. EBSD maps are color-coded with the IPF coloring in the sample normal direction Z_0. The inset is the color-coding legend.

bulk R_{sheet} values (25−150 Ω/□) through simple passivation with small polar molecules.

To further investigate the passivation effectiveness of ZK-series solutions, we worked specifically on samples passivated with ZK-42 solution with EBSD and PL. The PL image of a sample passivated with ZK-42 for 30 hours is shown in Figure **3a**. The contrast in a PL image is closely related to the defect density and lifetime in association with the material purity [28]. We can clearly see the GBs in the PL image due to their strong contrast with adjacent grain bulk. Also shown are the corresponding PL intensity profiles across GBs #1−3 indicated by arrows. The darkness of the three GBs follows the order GB #1 > GB #3 > GB #2 as far as the intensity counts are concerned: 55, 118, and 82 for GB #1, GB #2 and GB #3, respectively. In fact, we selected the three typical GBs #1−3 according to their different R_{sheet} values before passivation (6040.8, 138.2, and 3060.7 Ω/□ for GBs #1−3, respectively). We then measured the R_{sheet} under dark conditions at different passivation times (Figure **3b**). We see that the R_{sheet} values across GBs #1 and #3 decreased greatly after passivation for 10 hours and then became almost saturated with increasing passivation time, whereas the R_{sheet} across GB #2 was insensitive to passivation.

After passivation for 30 hours, the R_{sheet} values across GBs #1−3 are 503.7, 168.3, and 400.9 Ω/☐, respectively, which is consistent with the aforementioned intensity profile counts. To explain these findings, we further investigated the same GBs with plan-view EBSD mapping to observe the grain misorientation between two adjacent grains. Figure **3c** shows EBSD maps at GBs #1–3, respectively. The maps are color-coded with the inverse pole figure (IPF) coloring in the sample normal direction Z_0. Also shown is the grain misorientation (angle and axis of rotation) between adjacent grains. It indicates that GBs #1 and #3 are large-angle random GBs whereas GB #2 is a Σ3 coincidence site lattice (CSL) boundary. We therefore confirmed that our ZK-series solutions are very effective in passivating large-angle random GBs in *mc*-Si and do not passivate Σ3 GBs or deteriorate their electrical properties. These findings are consistent with those reported on GBs passivated with hydrogen [5]. In our recent study on upgraded metallurgical-grade silicon (UMG-Si) wafers, we also found a similar correlation between the optical response and different GBs passivated with a methanol–iodine solution [22]. However, we observed that methanol–iodine passivated *mc*-Si samples showed a wider range of PL imaging contrast for different GBs than ZK-series solution passivated ones, which further verified that our ZK-series solutions can effectively passivate random GBs.

To explain the passivation-enhanced conductivity of random GBs, we refer to a typical random GB model for *p*-type Si before passivation (Figure **4a**) [29]. As mentioned above, large-angle random GBs show high resistance for carriers to cross over, because high defects and impurity densities exist there [22]. These defects introduce extra electronic states localized within the band gap and act as trap states at GBs. When Fermi levels line up as a result of charge transfer to reach equilibrium, a potential barrier and interfacial polarization will be formed along the GB; the barrier will oppose the immigration of charge carriers. It is therefore reasonable that random GBs, in particular large-angle ones, show large R_{sheet} values. Tsurekawa *et al.* [30] showed that random boundaries possess barrier heights almost twice as high as those of coincidence boundaries. After passivation with ZK-series solutions, it is expected that the electric dipole moments of proper polar molecules in solutions and the interfacial dipole moments at the GB cancel each other out so that the GB potential barrier can be greatly lowered (Figure **4b**) and the corresponding R_{sheet} can be greatly reduced. Small molecules with high polarity was also applied in organic solar cells acting as both electron donor and acceptor to adjust interfacial energy barrier [31]. However, for pure solutions such as methanol, formic acid, and acetonitrile, we believe the molecular dipoles may not match with the interfacial dipoles at the GB, which leads to poor charge neutralization and passivation of polar molecules on localized charge states at GBs. It should be pointed out that the actual situation could be more complicated than the brief picture presented here. Therefore, more research work is needed to further clarify what actually happens at GBs during passivation; for instance, how deep small polar molecules can diffuse into GBs and how long they can stay there.

4. CONCLUSIONS

In summary, four-point probe, PL, and EBSD techniques were employed to study the passivation effect of small polar molecules on GBs in *mc*-Si wafers, including methanol, acetonitrile, formic acid, and new ZK-series solutions. It was shown that the ZK-series solutions have a much stronger passivation effect than others. The R_{sheet} across large-angle GBs could be

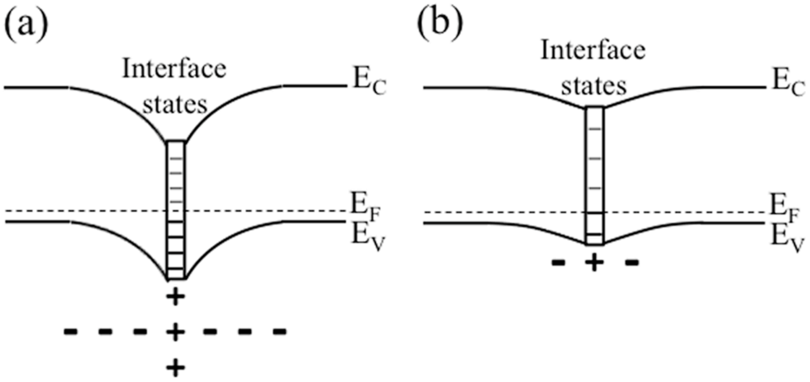

Figure 4: Random GB model. (**a**) Before passivation. (**b**) After passivation.

reduced by up to more than one order to be close to the bulk R_{sheet} (25−150 Ω/□) through simple passivation with ZK-series mixed solutions. In addition, we found an excellent correlation between the grain misorientation and passivation effectiveness. The results were explained with a GB model to be due to the effective charge neutralization and passivation of polar molecules on localized charge states at GBs. These findings are important because we believe that using non-hydrogen based approaches to passivation may help us achieve high-quality, economical semiconductor materials for photovoltaics and other solid-state devices such as thin-film transistors.

ACKNOWLEDGEMENTS

F. Liu acknowledges the financial support from the Seed Funding Programme for Basic Research at HKU (Project Codes 200910159016 and 201211159091), the University Development Fund (UDF) 2009-2010 (Second Round), and the HKU Initiative on Clean Energy & Environment (HKU-ICEE). W.C.H. Choy is grateful for the financial support of the General Research Fund (Grant Codes: HKU712010E and HKU711612E) from the Research Grants Council of Hong Kong Special Administrative Region, China. The authors also thank Yanfa Yan from the University of Toledo for stimulating discussion.

AUTHOR CONTRIBUTIONS

The manuscript was written through contributions of all authors. All authors have given approval to the final version of the manuscript.

REFERENCES

[1] Schropp REI, Carius R, Beaucarne G. Amorphous silicon, microcrystalline silicon and thin-film polycrystalline silicon solar cells. Mrs Bull 2007; 32: 219-224. http://dx.doi.org/10.1557/mrs2007.25

[2] Beaucarne G. Silicon Thin-Film Solar Cells. Advances in OptoElectronics 2007. http://dx.doi.org/10.1155/2007/36970

[3] Green MA. Crystalline and thin-film silicon solar cells: state of the art and future potential. Solar Energy 2003; 74: 181-192. http://dx.doi.org/10.1016/S0038-092X(03)00187-7

[4] Chen J, Yang D, Xi Z, Sekiguchi T. Recombination activity of Σ3 boundaries in boron-doped multicrystalline silicon: Influence of iron contamination. Journal of Applied Physics 2005; 97: 033701. http://dx.doi.org/10.1063/1.1836009

[5] Bertoni MI, Hudelson S, Newman BK, Fenning DP, Dekkers HFW, Cornagliotti E, *et al*. Influence of defect type on hydrogen passivation efficacy in multicrystalline silicon solar cells. Progress in Photovoltaics: Research and Applications 2011; 19: 187-191. http://dx.doi.org/10.1002/pip.1008

[6] Dimassi W, Derbali L, Bouaicha M, Bessais B, Ezzaouia H. Two-dimensional LBIC and Internal-Quantum-Efficiency investigations of grooved grain boundaries in multicrystalline silicon solar cells. Solar Energy 2011; 85: 350-355. http://dx.doi.org/10.1016/j.solener.2010.11.014

[7] Honda S, Mates T, Rezek B, Fejfar A, Kočka J. Microscopic study of the H_2O vapor treatment of the silicon grain boundaries. Journal of Non-Crystalline Solids 2008; 354: 2310-2313. http://dx.doi.org/10.1016/j.jnoncrysol.2007.09.107

[8] Seager CH, Ginley DS. Passivation of grain boundaries in polycrystalline silicon. Applied Physics Letters 1979; 34: 337-340. http://dx.doi.org/10.1063/1.90779

[9] Carnel L, Gordon I, Van Nieuwenhuysen K, Van Gestel D, Beaucarne G, Poortmans J. Defect passivation in chemical vapour deposited fine-grained polycrystalline silicon by plasma hydrogenation. Thin Solid Films 2005; 487: 147-151. http://dx.doi.org/10.1016/j.tsf.2005.01.081

[10] Dekkers HFW, Carnel L, Beaucarne G. Carrier trap passivation in multicrystalline Si solar cells by hydrogen from SiN:H layers. Applied Physics Letters 2006; 89: 013508. http://dx.doi.org/10.1063/1.2219142

[11] Darwiche S, Nikravech M, Morvan D, Amouroux J, Ballutaud D. Effects of hydrogen plasma on passivation and generation of defects in multicrystalline silicon. Solar Energy Materials and Solar Cells 2007; 91:195-200. http://dx.doi.org/10.1016/j.solmat.2006.08.008

[12] Nickel NH, Yin A, Fonash SJ. Influence of hydrogen and oxygen plasma treatments on grain boundary defects in polycrystalline silicon. Applied Physics Letters 1994; 65: 3099. http://dx.doi.org/10.1063/1.112449

[13] Rajesh C, Pramod MR, Patil S, Mahamuni S, More S, Dusane RO, *et al*. Reduction in surface recombination through hydrogen and 1-heptene passivated silicon nanocrystals film on silicon solar cells. Solar Energy 2012; 86: 489-495. http://dx.doi.org/10.1016/j.solener.2011.10.033

[14] Bousbih R, Dimassi W, Haddadi I, Ben Slema S, Rava P, Ezzaouia H. Silicon lifetime enhancement by SiNx:H anti-reflective coating deposed by PECVD using SiH_4 and N_2 reactive gas. Solar Energy 2012; 86: 1300-1305. http://dx.doi.org/10.1016/j.solener.2012.01.021

[15] Banerjee S, Sundaresan R, Shichijo H, Malhi S. Hot-electron degradation of n-channel polysilicon MOSFETs. IEEE Transactions on Electron Devices 1988; 35: 152-157. http://dx.doi.org/10.1109/16.2434

[16] Nickel NH, Jackson WB, Johnson NM. Light-induced creation of metastable paramagnetic defects in hydrogenated polycrystalline silicon. Physical Review Letters 1993; 71: 2733-2736. http://dx.doi.org/10.1103/PhysRevLett.71.2733

[17] Saad A, Mazanik A, Fedotov A, Partyka J, Węgierek P, Żukowski P. Influence of low-energy ion-beam treatment by hydrogen on electrical activity of grain boundaries in polycrystalline silicon. Vacuum 2005; 78: 269-272. http://dx.doi.org/10.1016/j.vacuum.2005.01.037

[18] Honda S, Mates T, Ledinský M, Fejfar A, Kočka J, Yamazaki T, *et al*. Defects generation by hydrogen passivation of polycrystalline silicon thin films. Solar Energy 2006; 80: 653-657. http://dx.doi.org/10.1016/j.solener.2005.10.013

[19] Huang-Chung C, Fang-Shing W, Huang CY. Effects of NH_3 plasma passivation on N-channel polycrystalline silicon thin-film transistors. IEEE Transactions on Electron Devices 1997; 44: 64-68. http://dx.doi.org/10.1109/16.554793

[20] Chhabra B, Bowden S, Opila RL, Honsberg CB. High effective minority carrier lifetime on silicon substrates using quinhydrone-methanol passivation. Applied Physics Letters

2010; 96: 063502.
http://dx.doi.org/10.1063/1.3309595

[21] Chhabra B, Weiland C, Opila RL, Honsberg CB. Surface characterization of quinhydrone–methanol and iodine–methanol passivated silicon substrates using X-ray photoelectron spectroscopy. physica status solidi (a) 2011; 208: 86-90.
http://dx.doi.org/10.1002/pssa.201026101

[22] Liu FD, Jiang CS, Guthrey H, Johnston S, Romero MJ, Gorman BP, *et al.* Optical response of grain boundaries in upgraded metallurgical-grade silicon for photovoltaics. Solar Energy Materials and Solar Cells 2011; 95: 2497-2501.
http://dx.doi.org/10.1016/j.solmat.2011.04.039

[23] Regan W, Byrnes S, Gannett W, Ergen O, Vazquez-Mena O, Wang F, *et al*. Screening-Engineered Field-Effect Solar Cells. Nano Letters 2012; 12: 4300-4304.
http://dx.doi.org/10.1021/nl3020022

[24] Zecca A, Chiari L, Sarkar A, Lima MAP, Bettega MHF, Nixon KL, *et al*. Positron scattering from formic acid. Physical Review A 2008; 78: 042707.
http://dx.doi.org/10.1103/PhysRevA.78.042707

[25] Kebarle P, Haynes RM, Collins JG. Competitive solvation of the hydrogen ion by water and methanol molecules studied in the gas phase. Journal of the American Chemical Society 1967; 89: 5753-5757.
http://dx.doi.org/10.1021/ja00999a003

[26] Wright D, Caldwell R, El-Shall MS. Vapor phase homogeneous nucleation of acetonitrile: the effect of dipole--dipole interaction. Chemical Physics Letters 1991; 176: 46-54.
http://dx.doi.org/10.1016/0009-2614(91)90008-W

[27] Bhattacharyya D, Shah D, Kissick K, Ghorpade A, Hannah R. Pervaporation of alcohol-water and dimethylformamide-water mixtures using hydrophilic zeolite NaA membranes: mechanisms and experimental results. Journal of Membrane Science 2000; 179: 185-205.
http://dx.doi.org/10.1016/S0376-7388(00)00515-9

[28] Schroder DK. Semiconductor Material and Device Characterization. 2nd ed: Wiley; 1998.

[29] Nelson J. The Physics of Solar Cells: Imperial College Press 2002.

[30] Tsurekawa S, Kido K, Watanabe T. Interfacial state and potential barrier height associated with grain boundaries in polycrystalline silicon. Materials Science and Engineering a-Structural Materials Properties Microstructure and Processing 2007; 462: 61-67.
http://dx.doi.org/10.1016/j.msea.2006.02.471

[31] Choi JW, Kulshreshtha C, Kennedy GP, Kwon JH, Jung S-H, Chae M. Solution-processed bulk heterojunction organic solar cells with high polarity small molecule sensitizer. Solar Energy Materials and Solar Cells 2011; 95: 2069-2076.
http://dx.doi.org/10.1016/j.solmat.2011.02.018

Received on 30-08-2014 Accepted on 23-09-2014 Published on 19-11-2014

DOI: http://dx.doi.org/10.15377/2410-2199.2014.01.01.2